Physics Letters B 820 (2021) 136569

Contents lists available at ScienceDirect

Physics Letters B

www.elsevier.com/locate/physletb

Structure of high-lying levels populated in the ^{96}Y $\rightarrow$ ^{96}Zr β decay

K.R. Mashtakov [a,b,i,*], V.Yu. Ponomarev [c], M. Scheck [a,b], S.W. Finch [d,e], J. Isaak [c], M. Zweidinger [c], O. Agar [f], C. Bathia [d,e], T. Beck [c], J. Beller [c], M. Bowry [a,b], R. Chapman [a,b], M.M.R. Chishti [a,b], U. Friman-Gayer [c,e,g], L.P. Gaffney [h], P.E. Garrett [i], E.T. Gregor [a,b], J.M. Keatings [a,b], U. Köster [j], B. Löher [k], A.D. MacLean [i], D. O'Donnell [a,b], H. Pai [c,l], N. Pietralla [c], G. Rainovski [m], M. Ramdhane [n], C. Romig [c], G. Rusev [d,e], D. Savran [k], G.S. Simpson [n], J. Sinclair [a,b], K. Sonnabend [j], P. Spagnoletti [a,b], A.P. Tonchev [d,e], W. Tornow [d,e]

[a] School of Computing, Engineering, and Physical Sciences, University of the West of Scotland, High Street, Paisley PA1 2BE, UK
[b] Scottish Universities Physics Alliance, University of Glasgow, University Avenue, Glasgow G12 8QQ, UK
[c] Institut für Kernphysik, TU Darmstadt, Schlossgartenstr. 9, 64289 Darmstadt, Germany
[d] Department of Physics, Duke University, Durham, NC 27708-0308, USA
[e] TUNL, Triangle Universities Nuclear Laboratory, Durham, NC 27708-0308, USA
[f] Department of Physics, Karamanoglu Mehmetbey University, 70100 Karaman, Turkey
[g] Department of Physics and Astronomy, University of North Carolina at Chapel Hill, Chappel Hill, NC 27599, USA
[h] Department of Physics, University of Liverpool, Liverpool L69 3BX, UK
[i] Department of Physics, University of Guelph, Guelph, Ontario N1G 2W1, Canada
[j] ILL, Institut Laue-Langevin, 71 avenue des Martyrs, 38000 Grenoble, France
[k] GSI Helmholtzzentrum für Schwerionenforschung GmbH, Darmstadt, 64289 Darmstadt, Germany
[l] Nuclear Physics Division, Saha Institute of Nuclear Physics, Kolkata, 700064, India
[m] Faculty of Physics, University of Sofia St. Kliment Ohridski, 1164 Sofia, Bulgaria
[n] LPSC, UJF Grenoble I, 53 avenue des Martyrs, 38026 Grenoble Cedex, France

ARTICLE INFO

Article history:
Received 31 October 2020
Received in revised form 24 June 2021
Accepted 31 July 2021
Available online 5 August 2021
Editor: B. Blank

This work is dedicated to the memory of Henryk Mach

Keywords:
High resolution gamma-ray spectroscopy
Pygmy dipole resonance
Reactor antineutrino anomaly
Quasi-particle phonon model

ABSTRACT

The nature of the high-lying final levels of the ^{96}Y$_{gs}$ β decay, one of the three most important contributors to the high-energy reactor antineutrino spectrum, has been investigated in high-resolution γ-ray spectroscopy following the β decay as well as in a campaign of inelastic photon scattering experiments. The comprehensive approach establishes 1^- levels associated with the Pygmy Dipole Resonance as high-lying final levels in the β decay. Branching ratios extracted from β decay complement photon scattering and allow the absolute $E1$ excitation strength to be determined for levels populated in both reactions. The combined data represents a comprehensive approach to the wavefunction of the 1^- levels below the Q_β value, which are investigated in the Quasiparticle Phonon Model. The calculations reveal that the components populated in β decay contribute only with small amplitudes to the complex wavefunction of these 1^- levels. A comparison of the β decay results to data from total absorption γ-ray spectroscopy demonstrates a good agreement between both measurements.

Following the observation of a lack of high-energy antineutrinos emitted from nuclear reactors [1], nuclear β-decay studies using total absorption γ-ray spectroscopy (TAGS) have shown that a larger number of β decays populate high-lying excited levels of the daughter nucleus (e.g., see Refs. [2,3] and references therein) than hitherto believed. Hence, the average energy shared by the emitted electron and antineutrino is less than previously anticipated from β-decay studies using high resolution γ-ray spectroscopy (HRS). While antineutrinos escape the reactor without further interaction, γ rays or conversion electrons emitted in the decay of these high-lying levels will be absorbed in the reactor and contribute to the heat production.

The underdetermined population of high-lying levels in previous β-decay studies can be attributed to the pandemonium effect [4]; that is, γ rays which are emitted in a γ-γ cascade are not

* Corresponding author at: Departments of Physics, University of Guelph, Guelph, Ontario, N1G 2W1, Canada.
E-mail addresses: kmastako@uoguelph.ca (K.R. Mashtakov), marcus.scheck@uws.ac.uk (M. Scheck).

https://doi.org/10.1016/j.physletb.2021.136569

recognised as such and are placed in the level scheme at too low energy or γ rays are not observed at all. A major source of this underdetermination is related to the detectors that have been previously used. Many of the earlier relevant β-decay studies used first generation semiconductor detectors with low γ-ray detection efficiency in comparison to what is currently available. This is particularly true for γ rays of comparatively high energy of several MeV. Meanwhile, TAGS has demonstrated the presence of this effect and quantified it to a good degree (e.g., see Ref. [5]). However, a task that is difficult to achieve with TAGS and its highly-efficient scintillator detectors, but limited energy resolution is to clarify the nature of the populated levels.

Therefore, HRS is necessary to identify the populated levels and to determine their spectroscopic properties. In order to explore the nature of these levels, it is also beneficial to investigate them with complementary reactions; however, due to the high level density above about 3 MeV, this is a difficult task. For β decays originating from mother nuclei with low ground-state spin, an ideal combination of population processes was identified in Ref. [6]. There, β decay was used to populate levels associated with the Pygmy Dipole Resonance (PDR) [7,8], an accumulation of strongly excited 1^- levels on the low-energy tail of the Giant Dipole Resonance (GDR) [9,10]. A standard tool to investigate these 1^- levels in stable nuclei is the resonant scattering of real photons, the so-called nuclear resonance fluorescence (NRF) [11]. Because of the low associated angular momentum transfer, which is almost entirely limited to the $1\hbar$ intrinsic angular momentum of the photon, the (γ,γ') reaction selectively populates 1^π levels and permits γ-ray spectroscopy in energy regimes with a high level density. Another advantage is that the NRF scattering process is solely governed by the well-understood electromagnetic interaction. Hence, in addition to the complex β-decay matrix element connecting the mothers ground state and the excited level in the daughter, for many levels the wavefunction is tested with the electromagnetic matrix element connecting the ground state of the daughter and the excited level.

Interestingly, the three main contributors [12] to the reactor high-energy antineutrino spectrum, ^{92}Rb ($Q_\beta = 8095(6)$ keV) [13], ^{96}Y ($Q_\beta = 7096(23)$ keV) [14], and ^{142}Cs ($Q_\beta = 7308(11)$ keV) [15] all have a 0^- ground state. Consequently, it can be expected that, in the daughter, mainly 1^- levels are populated via Gamow-Teller β decays, exactly the type of levels that are populated in the NRF of their even-even daughter nuclei. However, the NRF cross sections are comparatively low and given the available photon flux at current facilities, the target material required limits the applicability to (quasi-)stable isotopes. For this reason, the β decay of ^{96}Y to its stable daughter ^{96}Zr was investigated, and the combined results have been interpreted within the Quasi-particle Phonon Model (QPM) [16].

The β-decay experiment was performed following the neutron-induced fission of ^{235}U at the research reactor of the Institut Laue Langevin (ILL). Fission fragments were mass separated using the LOHENGRIN separator [17] and transported to a setup consisting of a cooled lithium-doped silicon detector used for the detection of electrons, two high-efficiency Clover (HPGe) germanium detectors in close geometry and two further single-crystal HPGe detectors. This approach allowed the measurement of electron-γ and γ-γ coincidences. The extracted data will benefit the TAGS measurement for this particular decay, since the TAGS measurement was not sensitive to the 1581-keV $0_2^+ \rightarrow 0_{gs}^+$ $E0$ decay [18] from the first excited level in ^{96}Zr. The mass separation of LOHENGRIN is not sufficient to distinguish between the 0^- ground state and the 8^+ isomeric state of the ^{96}Y mother. For levels in ^{96}Zr below 4 MeV it was necessary to rely on the β-decay data from Ref. [19], which does distinguish decays from the 0^- and 8^+ states. In addition to available spectroscopic information, the distinct decay behaviour

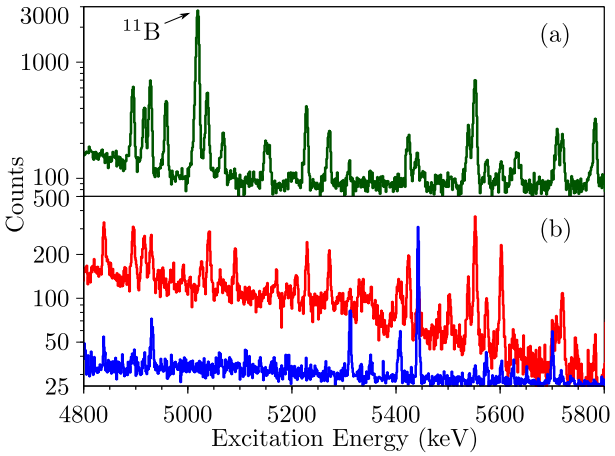

Fig. 1. Partial γ-ray spectra recorded in the ^{96}Zr(γ,γ') reaction (a) and ^{96}Y$_{gs}$ β decay (b). The upper (red) spectrum in part (b) is an electron-gated projection of the e^--γ matrix. The lower (blue) spectrum is gated on the $0_2^+ \rightarrow 0_{gs}^+$-$E0$ transition depopulating the first excited level in ^{96}Zr. The $E0$-gated spectrum has been shifted by the excitation energy of the 0_2^+ level, so that the peaks appear at the level energy. This procedure allows to identify transitions stemming from the same level. Note the log-scale of the y axis.

of levels populated by these very different spins allows an association of γ rays originating from levels above 4 MeV with the ^{96}Y ground-state decay. The data from Ref. [19] as well as other sources (e.g., the β decay of ^{86}Br [20]) were used for an internal efficiency calibration. In previous HRS β-decay measurement the first-generation single-crystal Ge detectors with relative efficiency of $\epsilon = 26\%$ [19] were used while the present HRS study was equipped with two Clover detectors each consisting of four 50×80 mm HPGe crystals with the combined relative efficiency of $\epsilon \approx 150\%$ per one Clover in the add-back regime [21]. The improved overall γ-ray detection efficiency resulted in the identification of 36 newly observed levels, 17 direct ground-state decays and 15 γ-ray transitions branching to the lower-lying excited states. The majority of the newly observed beta-feedings have intensity values below 0.01%, which also demonstrates the enhanced sensitivity of the current measurement. While the overall recovered β-feeding intensity to the levels above 4 MeV is relatively low ($\sum I_\beta \approx 0.27\%$), the new HRS measurement extends and rebalances the β-feeding pattern in this energy region.

The ^{96}Zr(γ,γ') NRF campaign used continuous bremsstrahlung beams at the DHIPS setup [22] of the S-DALINAC as well as quasi-monochromatic ($\Delta E_\gamma / E_\gamma \approx 3\%$) fully-polarised photon beams at the High Intensity γ-ray Source (HI$\vec{\gamma}$S) [23] in the entrance channel. For the experiments performed at DHIPS a ^{96}Zr target enriched to 95.63% was used, while a 91.39% enriched 7.28 g ZrO_2 target was employed in experiments at HI$\vec{\gamma}$S. From this campaign the spin and parity of the NRF excited levels were unambiguously determined and their integrated scattering cross sections measured. Fig. 1 shows parts of the spectra recorded in the ^{96}Zr(γ,γ') reaction [part (a)] and following the ^{96}Y$_{gs}$ β decay [part (b)]. More details about the experiments, setups, data analysis, and the final data tables will be reported in a following publication.

In Fig. 2, the level population in β decay [part (b)] is compared to the excitation strength of levels observed in NRF [part (a)] up to 6.5 MeV. From the part of the NRF campaign that used fully-polarised γ rays in the entrance channel, for all levels above 4.5 MeV excited in this reaction, including 14 newly observed states populated in both β-decay and NRF reactions, a firm spin and parity assignment of 1^- has been made. This observation agrees with the expectation that most levels observed in β decay are populated in Gamow-Teller allowed decays from the 0^- ground

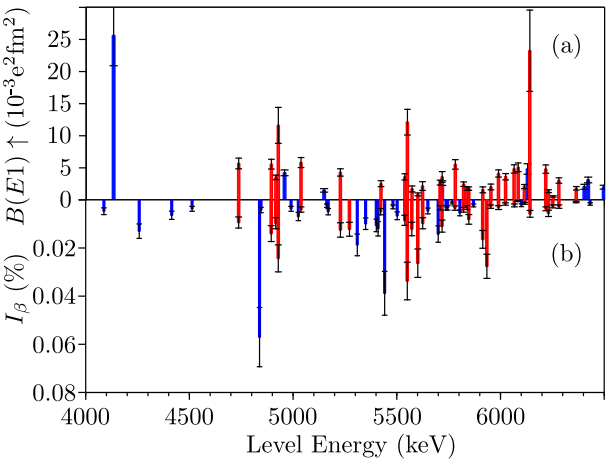

Fig. 2. Comparison of the ^{96}Zr $B(E1)$-strength distribution observed in the NRF reaction [part (a)] and the population-intensity distribution in β decay from ^{96}Y$_{gs}$ [part (b)]. Levels that are populated in both reactions are given as red bars and levels that are solely observed in one reaction as blue bars. The results from NRF were corrected for the branching ratios observed in β decay.

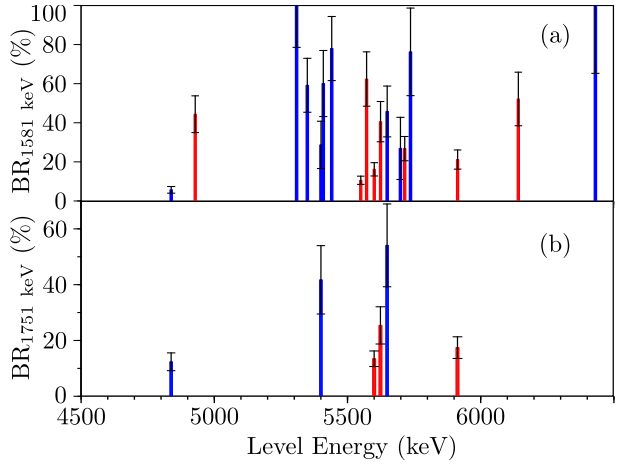

Fig. 3. Branching ratios to the first excited 0_2^+ level at 1581 keV [part (a)], and the first excited 2_1^+ level at 1751 keV [part (b)] as extracted from the present β-decay measurement. Levels observed in both NRF and β decay are marked with red bars. Levels that were solely observed in β decay are marked as blue bars. Note the different scales on the y axis.

state of ^{96}Y. Almost all levels observed in NRF were also observed in β decay.

Due to the large background in NRF spectra stemming from non-resonant scattered photons, which increases exponentially to lower energies, branching transitions are often below the sensitivity limit. Consequently, the excitation probabilities in the NRF data are underestimated. The $B(E1)$ excitation strengths shown in Fig. 2 include the branching ratio data from β decay. Fig. 3 shows the branching ratios for the two low-lying excited levels that are most frequently populated. Hence, apart from a few levels with a $B(E1)$ strength below the sensitivity limit, the data presented in Fig. 2 (a) resembles the true excitation pattern up to 6.4 MeV.

The level population probability in β decay extracted from the present HRS measurement (in combination with the data from Ref. [19]) and the data obtained in the TAGS work [18] are compared in Fig. 4. In order to be able to compare the results, the data of HRS and TAGS are given in 100 keV bins. Remarkably, both methods result in overall good agreement. The two most striking differences are groups of levels near 3 and 4 MeV in the TAGS spectrum and the very high-lying levels that were not seen in HRS.

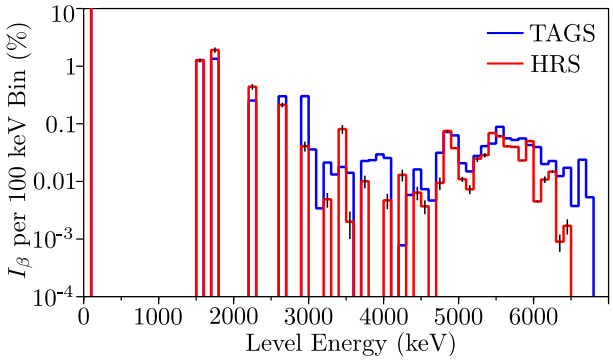

Fig. 4. Comparison of level population intensity as a function of excitation energy between the results from total absorption γ-ray spectroscopy [18] (TAGS, blue) and the combination of the presented work and data published in Ref. [19] for high-resolution γ-ray spectroscopy (HRS, red). The y-axis has been truncated at 10% to improve the display of the data. The ground state to ground state β-feeding value corresponds to 95.5(5)% as measured in [18] and [19]. For a discussion see text.

As shown in Fig. 3 (a) in HRS several levels, especially a group of levels near 5.5 MeV, strongly branch to the first excited 0_2^+ level at 1581 keV. Since the TAGS measurement reported in Refs. [2,18] was not sensitive to the subsequent $E0$ transition, these γ rays were placed at a too low energy. The non-observation of the very high-lying levels in HRS has sensitivity issues. The summed singles γ-ray spectrum from all HPGe detectors was contaminated with a large background stemming from the nearby reactor. In order to suppress the uncorrelated background, this work used e^--γ coincidences. However, the threshold of the silicon electron detector was set at a comparably high energy of ≈300 keV and, consequently, a large fraction of the β-particle spectrum corresponding to decays to levels near the Q_β value lies below the energy threshold and was not included. Hence, the e^--γ coincidence efficiency was too low for these weakly-populated levels to be observed. For only one level in this region a γ ray was present in the γ-γ matrix, consequently, it can be concluded that the other levels depopulate exclusively to the ground state. Nevertheless, Fig. 4 demonstrates that HRS using modern highly-efficient HPGe detector arrays is capable of resolving the pandemonium effect in ^{96}Zr and possibly in two other most important contributors to the high-energy reactor antineutrino spectrum. Furthermore, the combined approach of HRS and NRF establishes the 1^- levels of the PDR as final states of the ^{96}Y$_{gs}$ β decay.

In the following, the properties of the 1^- states in ^{96}Zr are investigated in the QPM [16,24]. In the QPM, phonons are composed of one-particle one-hole (1p1h) configurations. Their excitation energies and corresponding internal fermionic structure is obtained from solving the QRPA equations. The model calculations have been performed with wavefunctions that contain one-, two-, and three-phonon configurations. For computational reasons, the configurations above 25.0, 21.0, and 9.7 MeV, respectively, have been truncated. This truncation allows a consideration of the fragmentation of the excitation strength in a wide energy interval including the GDR and at the same time allows a study of the fine structure of the PDR in more detail. While many 1p1h configurations have a non-zero matrix element for Eλ transitions and, accordingly, contribute to the $B(E\lambda)$ value for one-phonon components of the wavefunction, the population of one-phonon components in the β-decay of odd-odd nuclei is very selective to only a few one-phonon (1p1h) configurations and two-phonon (2p2h) excitations. As already discussed in Refs. [6,25,26], excited states of even-even nuclei are predominantly populated in the electromagnetic excitation from the ground state via one-phonon components of their wavefunctions; two-phonon configurations are excited much more

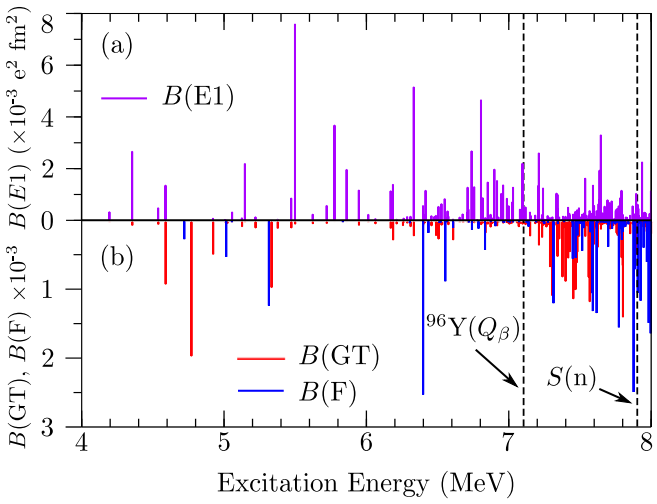

Fig. 5. The upper part shows the $B(E1)$-strength distribution of ^{96}Zr as calculated in the quasiparticle phonon model. In the lower part the calculated Fermi, $B(F)$, (blue) and Gamow-Teller, $B(GT)$, (red) strength distributions for the ^{96}Y $\rightarrow$^{96}Zr β decay are shown. The energy range is limited to just above the experimentally accessibly regions of Q_β value and neutron-separation threshold $S(n)$. For a discussion see text.

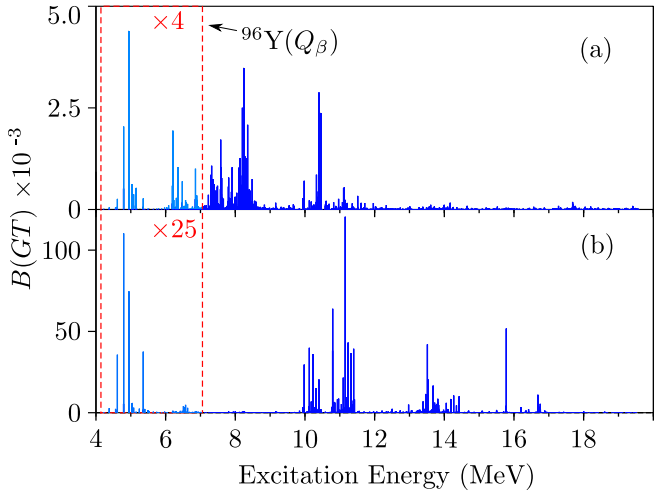

Fig. 6. Gamow-Teller strength distribution $B(GT)$ of the ^{96}Y $\rightarrow$^{96}Zr β decay disentangled whether one-phonon (1p1h) [part a)] or two-phonon (2p2h) [part b)] components are populated in the wavefunction of the final 1^- level. For a clarity of the presentation the scales on the y-axis were adjusted distinguishing whether one- or two-phonon components are populated. Furthermore, for the energy range below Q_β light blue bars were multiplied by the given factors. The total calculated low-energy $B(GT)$ strength, which includes the interference of the components, is shown in Fig. 5 (b).

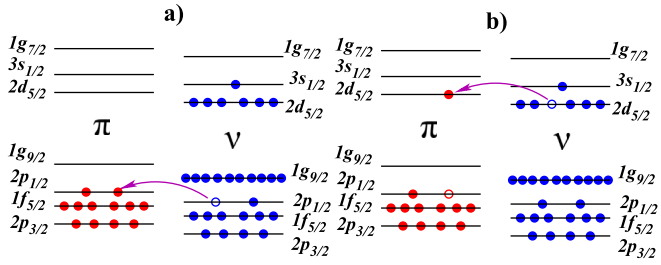

Fig. 7. Schematic representation of the shell structure involved in the ^{96}Y β decay. Part a) shows the decay to the neutron $\{2p^{-1}_{1/2} \times 3s_{1/2}\}_\nu$ one-particle one-hole configuration and part b) the decay resulting in a proton $\{2p^{-1}_{1/2} \times 2d_{5/2}\}_\pi$ and neutron $\{2d^{-1}_{5/2} \times 3s_{1/2}\}_\nu$ two-particle two-hole configuration. Particles are shown as full circles, while holes are represented by open circles.

weakly (except for the collective $[2^+_1 \otimes 3^-_1]_{1^-}$ state) and form a kind of a structureless "background".

In the calculation, we assume the wavefunction of the ^{96}Y ground state as a pure $\{\nu 3s_{1/2} \times \pi 2p_{1/2}\}_{0^-}$ configuration (a schematic shell structure is shown in Fig. 7). This assumption is confirmed by a microscopic quasi-particle random phase approximation (QRPA) calculation, which yields more than a 99% contribution of this configuration to the wavefunction of the first 0^- state in ^{96}Y. Interestingly, in order to couple to $J = 0$, the spins of proton and neutron must align to $S = 1$. 95.6% of all β decays [2,19] proceed to the ground state of ^{96}Zr. In this first-forbidden decay [27], the neutron in the $\nu 3s_{1/2}$ subshell decays with a spin-flip to the proton $\pi 2p_{1/2}$ subshell.

The calculated low-energy part of the $B(E1)$-strength distribution in ^{96}Zr is presented in Fig. 5 (a) and Fig. 5 (b) provides the calculated Fermi $B(F)$ and Gamow-Teller $B(GT)$ transition strength from the 0^- ground state of ^{96}Y to the same set of 1^- states in ^{96}Zr. While the calculation predicts several 0^- levels below Q_β, a search in the γ-γ matrix for $E1/M1$ decays to low-lying $1^+/1^-$ levels did not reveal any experimental candidates for 0^- levels below Q_β. Instead the experiment establishes that the population of levels above 4 MeV exclusively proceeds to 1^- levels via GT decays. To include GT decays, the QPM approach [6] had to be extended.

The Fig. 6 demonstrates the Gamow-Teller transition probabilities to the one- and two-phonon states predicted for the ground-state β decay of ^{96}Y over a wide energy range. It becomes immediately evident that only a small fraction of the total $B(GT)$ strength may be observed in the β-decay experiments for energy reasons. Additionally, due to the selective nature of the β decay population mechanism, the GT transition probabilities to the one-phonon components of 1^- states are significantly lower compared to the probability of populating two-phonon configurations. For the ^{96}Y$\rightarrow$^{96}Zr Gamow-Teller decay the most relevant 1p1h configurations are: $\{2p^{-1}_{1/2} \times 3s_{1/2}\}_\pi$ at 10.1 MeV, $\{2p^{-1}_{1/2} \times 3s_{1/2}\}_\nu$ at 8.8 MeV, and $\{2p^{-1}_{3/2} \times 3s_{1/2}\}_\nu$ at 10.5 MeV, which correspond to the decays $3s_{1/2} \rightarrow 3s_{1/2}$, $2p_{1/2} \rightarrow 2p_{1/2}$, and $2p_{3/2} \rightarrow 2p_{1/2}$, respectively. A visualisation for the decay leaving the daughter in the $\{2p^{-1}_{1/2} \times 3s_{1/2}\}_\nu$ 1p1h configuration is shown in Fig. 7 a) and an example for the population of a two-phonon component, corresponding to a 2p2h excitation, is shown in Fig. 7 b). The residual interaction of the nuclear Hamiltonian mixes these configurations in the set of one-phonon 1^- states and the coupling to multiple further two- and three-phonon configurations leads to the damping of the GT strength.

At the same time, the model provides a reasonable fragmentation of the Gamow-Teller strength and the absolute $B(GT)$ values at low energies (see Fig. 5 (b)). In order to explore the contribution of the component populated in β decay to the total wavefunction of a 1^- state, we use the example of the 1^- level at 4.838(1) MeV with an experimental $\log ft = 6.64(10)$. Both the calculated energy of 4.895 MeV as well as $\log ft = 6.66$ (calculated with $g_A/g_V = 1.23$ [28]) are in excellent agreement. In experiment and theory this level is the strongest populated level in β decay but not populated by photons. Interestingly, the wavefunction of this state is dominated by a large number of two- (2p2h) and three-phonon (3p3h) configurations which cannot be populated in β decay. The sheer number of particle-hole components with significant contributions to the wavefunctions of this state may also serve as an indication of the collective nature. The $\{2d^{-1}_{5/2} \times 3s_{1/2}\}_\nu\{2p^{-1}_{3/2} \times 1g_{9/2}\}_\pi$ and $\{2d^{-1}_{5/2} \times 3s_{1/2}\}_\nu\{2d^{-1}_{5/2} \times 1h_{11/2}\}_\pi$ two-phonon configurations are the two most dominant components with the corresponding relative contributions of 18.5% and 12.1% to the amplitude of the wavefunction. On the contrary, the $\{2d^{-1}_{5/2} \times 3s_{1/2}\}_\nu\{2p^{-1}_{1/2} \times 2d_{5/2}\}_\pi$ two-phonon component,

which is populated in the $\nu 2d_{5/2} \rightarrow \pi 2d_{5/2}$ β decay, contributes only 0.27% to the normalisation of the wavefunction. The wavefunctions of the other levels demonstrate that the astonishingly small contribution of the component(s) populated in β decay is a general feature. However, even this small component in the wavefunction is sufficient that the β-decay matrix element to the high-lying levels can compete with lower-lying levels, for which the phase-space factor is enhanced.

In summary, in the energy range below Q_β almost all 1^- levels that are excited in the (γ, γ') reaction are populated in β decay, too. This observation demonstrates the role of the PDR in the population of higher-lying levels in the $^{96}Y_{gs}$ β decay, which is an important contributor to the reactor high-energy antineutrino spectrum. This work demonstrates that HRS with modern arrays is capable to resolve the pandemonium for the three most important contributors to the reactor antineutrino energy spectrum in the 5-7 MeV range and emancipates HRS as partner of TAGS measurements to address the lack of high-energy reactor antineutrinos. The investigation of the microscopic structure of the observed levels in the QPM resulted in a good agreement with experiment. Interestingly, the QPM demonstrates that the components of the 1^- PDR levels, which are populated in β decay, contribute with only small amplitudes to the overall wavefunction.

Declaration of competing interest

The authors declare that they have no known competing financial interests or personal relationships that could have appeared to influence the work reported in this paper.

Acknowledgements

The authors acknowledge the generous offer by B.C. Rasco to provide the data for the TAGS measurement used in Fig. 4. The UK authors acknowledge financial support by the UK-STFC (Grant No. ST/P005101/1). This work is supported by the Deutsche Forschungsgemeinschaft through Grant No. SFB-634 (Project ID 5465852) and SFB-1245 (279384907) and by the U.S. Department of Energy (DOE), Office of Nuclear Physics, under grant No. DE-FG02-97ER41033. J.I. and N.P. acknowledge support by the state of Hesse under grant Nuclear Photonics by the LOEWE program. H.P. is grateful for the support of the Ramanujan Fellowship research grant under SERB-DST (SB/S2/RJN-031/2016).

References

[1] F.P. An, et al., Daya Bay Collaboration, Phys. Rev. Lett. 116 (2016) 061801, https://doi.org/10.1103/PhysRevLett.116.061801.
[2] B. Rasco, M. Wolińska-Cichocka, A. Fijałkowska, K.P. Rykaczewski, M. Karny, R.K. Grzywacz, K. Goetz, C.J. Gross, D.W. Stracener, E. Zganjar, et al., Phys. Rev. Lett. 117 (2016) 092501.
[3] V. Guadilla, A. Algora, J.L. Tain, M. Estienne, M. Fallot, A.A. Sonzogni, J. Agramunt, J. Äystö, J.A. Briz, A. Cucoanes, T. Eronen, L.M. Fraile, E. Ganioğlu, W. Gelletly, D. Gorelov, J. Hakala, A. Jokinen, D. Jordan, A. Kankainen, V. Kolhinen, J. Koponen, M. Lebois, L.L. Meur, T. Martinez, M. Monserrate, A. Montaner-Pizá, I. Moore, E. Nácher, S.E. Orrigo, H. Penttilä, I. Pohjalainen, A. Porta, J. Reinikainen, M. Reponen, S. Rinta-Antila, B. Rubio, K. Rytkönen, T. Shiba, V. Sonnenschein, E. Valencia, V. Vedia, A. Voss, J.N. Wilson, A.A. Zakari-Issoufou, Phys. Rev. Lett. 122 (2019) 042502, https://doi.org/10.1103/PhysRevLett.122.042502.
[4] J.C. Hardy, L.C. Carraz, B. Jonson, P.G. Hansen, Phys. Lett. B 71 (1977) 307–310, https://doi.org/10.1016/0370-2693(77)90223-4.
[5] M. Estienne, M. Fallot, A. Algora, J. Briz-Monago, V.M. Bui, S. Cormon, W. Gelletly, L. Giot, V. Guadilla, D. Jordan, L.L. Meur, A. Porta, S. Rice, B. Rubio, J.L. Taín, E. Valencia, A.A. Zakari-Issoufou, Phys. Rev. Lett. 123 (2019) 022502, https://doi.org/10.1103/PhysRevLett.123.022502.
[6] M. Scheck, S. Mishev, V.Y. Ponomarev, R. Chapman, L.P. Gaffney, E.T. Gregor, N. Pietralla, P. Spagnoletti, D. Savran, G.S. Simpson, Phys. Rev. Lett. 116 (2016) 132501, https://doi.org/10.1103/PhysRevLett.116.132501.
[7] D. Savran, T. Aumann, A. Zilges, Prog. Part. Nucl. Phys. 70 (2013) 210–245, https://doi.org/10.1016/j.ppnp.2013.02.003.
[8] A. Bracco, E.G. Lanza, A. Tamii, Prog. Part. Nucl. Phys. 106 (2019) 360–433, https://doi.org/10.1016/j.ppnp.2019.02.001.
[9] P.F. Bortignon, A. Bracco, R.A. Broglia, Giant Resonances, Routledge, 2019.
[10] M.N. Harakeh, A. Woude, Giant Resonances: Fundamental High-Frequency Modes of Nuclear Excitation, vol. 24, Oxford University Press on Demand, 2001.
[11] U. Kneissl, H.H. Pitz, A. Zilges, Prog. Part. Nucl. Phys. 37 (1996) 349–433, https://doi.org/10.1016/0146-6410(96)00055-5.
[12] A.A. Sonzogni, T.D. Johnson, E.A. McCutchan, Phys. Rev. C 91 (2015) 011301, https://doi.org/10.1103/PhysRevC.91.011301.
[13] C.M. Baglin, Nucl. Data Sheets 113 (2012) 2187–2389, https://doi.org/10.1016/j.nds.2012.10.001.
[14] D. Abriola, A.A. Sonzogni, Nucl. Data Sheets 109 (2008) 2501–2655, https://doi.org/10.1016/j.nds.2008.10.002.
[15] T.D. Johnson, D. Symochko, M. Fadil, J.K. Tuli, Nucl. Data Sheets 112 (2011) 1949–2127, https://doi.org/10.1016/j.nds.2011.08.002.
[16] V.G. Soloviev, Theory of Atomic Nuclei, Quasi-Particle and Phonons, CRC Press, 1992.
[17] P. Armbruster, M. Asghar, J.P. Bocquet, R. Decker, H. Ewald, J. Greif, E. Moll, B. Pfeiffer, H. Schrader, F. Schussler, G. Siegert, H. Wollnik, Nucl. Instrum. Methods 139 (1976) 213–222, https://doi.org/10.1016/0029-554X(76)90677-7.
[18] B. Rasco, A. Fijałkowska, K. Rykaczewski, M. Wolińska-Cichocka, M. Karny, R. Grzywacz, K. Goetz, C. Gross, D. Stracener, E. Zganjar, J. Batchelder, J. Blackmon, N. Brewer, T. King, K. Miernik, S. Paulauskas, M. Rajabali, J. Winger, Acta Phys. Pol. B 48 (2017) 507, https://doi.org/10.5506/APhysPolB.48.507.
[19] H. Mach, E.K. Warburton, R.L. Gill, R.F. Casten, J.A. Becker, B.A. Brown, J.A. Winger, Phys. Rev. C 41 (1990) 226–242, https://doi.org/10.1103/PhysRevC.41.226.
[20] A. Negret, B. Singh, Nucl. Data Sheets 124 (2015) 1–156, https://doi.org/10.1016/j.nds.2014.12.045.
[21] M. Jentschel, A. Blanc, G. de France, U. Köster, S. Leoni, P. Mutti, G. Simpson, T. Soldner, C. Ur, W. Urban, et al., J. Instrum. 12 (2017) P11003, https://doi.org/10.1088/1748-0221/12/11/p11003.
[22] K. Sonnabend, D. Savran, J. Beller, M.A. Büssing, A. Constantinescu, M. Elvers, J. Endres, M. Fritzsche, J. Glorius, J. Hasper, J. Isaak, B. Löher, S. Müller, N. Pietralla, C. Romig, A. Sauerwein, L. Schnorrenberger, C. Wälzlein, A. Zilges, M. Zweidinger, Nucl. Instrum. Methods Phys. Res. A 640 (2011) 6–12, https://doi.org/10.1016/j.nima.2011.02.107.
[23] H.R. Weller, M.W. Ahmed, H. Gao, W. Tornow, Y.K. Wu, M. Gai, R. Miskimen, Prog. Part. Nucl. Phys. 62 (2009) 257–303, https://doi.org/10.1016/j.ppnp.2008.07.001.
[24] N.L. Iudice, V.Y. Ponomarev, C. Stoyanov, A.V. Sushkov, V.V. Voronov, J. Phys. G, Nucl. Part. 39 (2012) 043101, https://doi.org/10.1088/0954-3899/39/4/043101.
[25] R.D. Herzberg, P.V. Brentano, J. Eberth, J. Enders, R. Fischer, N. Huxel, T. Klemme, P.V. Neumann-Cosel, N. Nicolay, N. Pietralla, V.Y. Ponomarev, J. Reif, A. Richter, C. Schlegel, R. Schwengner, S. Skoda, H.G. Thomas, I. Wiedenhöver, G. Winter, A. Zilges, Phys. Lett. B 390 (1997) 49–54, https://doi.org/10.1016/S0370-2693(96)01374-3.
[26] V.Y. Ponomarev, C. Stoyanov, N. Tsoneva, M. Grinberg, Nucl. Phys. A 635 (1998) 470–483, https://doi.org/10.1016/S0375-9474(98)00187-0.
[27] L. Hayen, J. Kostensalo, N. Severijns, J. Suhonen, Phys. Rev. C 100 (2019) 054323, https://doi.org/10.1103/PhysRevC.100.054323.
[28] A. Bohr, B.R. Mottelson, Nuclear Structure. Volume I. Single-Particle Motion, 1969.